DIFFERENT POWER-LAW INDICES IN THE FREQUENCY DISTRIBUTIONS OF FLARES WITH AND WITHOUT CORONAL MASS EJECTIONS

S. YASHIRO,[1,2] S. AKIYAMA,[1,2] N. GOPALSWAMY,[2] AND R. A. HOWARD[3]

ABSTRACT

We investigated the frequency distributions of flares with and without coronal mass ejections (CMEs) as a function of flare parameters (peak flux, fluence, and duration of soft X-ray flares). We used CMEs observed by the Large Angle and Spectrometric Coronagraph (LASCO) on board the *Solar and Heliospheric Observatory* (*SOHO*) mission and soft X-ray flares (C3.2 and above) observed by the *Geostationary Operational Environmental Satellite* (*GOES*) during 1996–2005. We found that the distributions obey a power law of the form $dN/dX \propto X^{-\alpha}$, where X is a flare parameter and dN is the number of events recorded within the interval $[X, X + dX]$. For the flares with (without) CMEs, we obtained the power-law index $\alpha = 1.98 \pm 0.05$ ($\alpha = 2.52 \pm 0.03$) for the peak flux, $\alpha = 1.79 \pm 0.05$ ($\alpha = 2.47 \pm 0.11$) for the fluence, and $\alpha = 2.49 \pm 0.11$ ($\alpha = 3.22 \pm 0.15$) for the duration. The power-law indices for flares without CMEs are steeper than those for flares with CMEs. The larger power-law index for flares without CMEs supports the possibility that nanoflares contribute to coronal heating.

Subject headings: Sun: corona — Sun: coronal mass ejections (CMEs) — Sun: flares

1. INTRODUCTION

Heating of the solar corona is one of the fundamental problems in solar physics. Solar flares have been proposed as a heat source, but the observed flares do not supply enough energy to keep the coronal temperature at a million degrees. However, tiny flares known as nanoflares, whose intensity is below the observational limits, may be able to heat the corona (Parker 1988). Since the nanoflares cannot be detected as discreet events with the current observational capability, their occurrence frequency distribution is often extrapolated from the observed flares. The flare frequency distributions can be represented by a power law of the form $dN/dE \propto E^{-\alpha}$, where E is flare energy and dN is the number of events recorded within the interval $[E, E + dE]$. When $\alpha < 2$, only larger flares predominantly contribute to coronal heating (Hudson 1991), meaning that nanoflares cannot contribute. Flare peak flux or peak count rate have been used to obtain the power-law index since it is difficult to measure the total flare energy. Many authors have examined α for various parameters of flares and flare-related phenomena and found α to be smaller than 2 (e.g., Crosby et al. 1993; Aschwanden et al. 1998 and references therein). The only exception was for quiet-region flares observed in EUV ($\alpha = 2.3$–2.6; Krucker & Benz 1998).

After the discovery of CMEs in 1971, the relation between flares and CMEs has been studied extensively (see Kahler 1992 for review). A close relation is also indicated from the similarity between the derivative of the X-ray light curve and CME acceleration profile (Zhang et al. 2001; Vršnak et al. 2004). However, not all flares are associated with CMEs. Even X-class flares (about 10% of them) lack CME association (Yashiro et al. 2005). Since a large, uniform, and extended database on CMEs has become available for the first time from *SOHO*, we can perform an extensive statistical analysis for a detailed examination of flares with and without CMEs. In this Letter, we show the frequency distributions for flares with and without CMEs, and we discuss their implications for the problems of coronal heating.

2. DATA SET

The basic flare parameters such as peak flux, fluence, and duration are available in the solar geophysical data (SGD) and online solar event reports[4] provided by the NOAA. The peak flux, measured in the 0.1–0.8 nm wavelength band, determines the rank of X-ray flares. The letters (A, B, C, M, X) designate the order of magnitude of the peak flux (10^{-8}, 10^{-7}, 10^{-6}, 10^{-5}, and 10^{-4} W m^{-2}, respectively). The number following the letter is the multiplicative factor. For example, an M3.2 flare indicates an X-ray peak flux of 3.2×10^{-5} W m^{-2}. The fluence (total flux) of a flare is obtained by integrating the X-ray flux in the 0.1–0.8 nm band from its start to end. No background subtraction is applied for the peak flux and fluence. The flare start time is identified as the first minute in a sequence of 4 minutes of steep monotonic increase in 0.1–0.8 nm flux. The end time corresponds to the time when the flux decays to a point halfway between the maximum flux and the preflare background level. More than 20,000 flares have been recorded from 1996 to 2005, but not all events were used in this study. We excluded flares below C3.2 level, since it is very difficult to examine their CME association. In this Letter, a C-class flare means the peak flux is between C3.2 and C9.9 level.

We used CME data routinely obtained by the C2 and C3 telescopes of LASCO (Brueckner et al. 1995) on board *SOHO*. We excluded flares corresponding to *SOHO* LASCO downtimes. For the CME occurrence rate studies, usually a 3 hr criterion is used to define LASCO downtimes (St. Cyr et al. 2000; Gopalswamy et al. 2004), but we applied a harder criterion in this study. We required at least two LASCO C2 images were obtained between 0 and 2 hr after the flare onset. Examining the CME visibility (detection efficiency) of the LASCO coronagraphs, Yashiro et al. (2005) found that about half of disk CMEs associated with C-class flares and ~16% of disk CMEs associated with M-class flares were invisible to LASCO, while all CMEs associated with X-class flares were

---

[1] Catholic University of America, Washington, DC 20064.
[2] NASA Goddard Space Flight Center, Greenbelt, MD 20771.
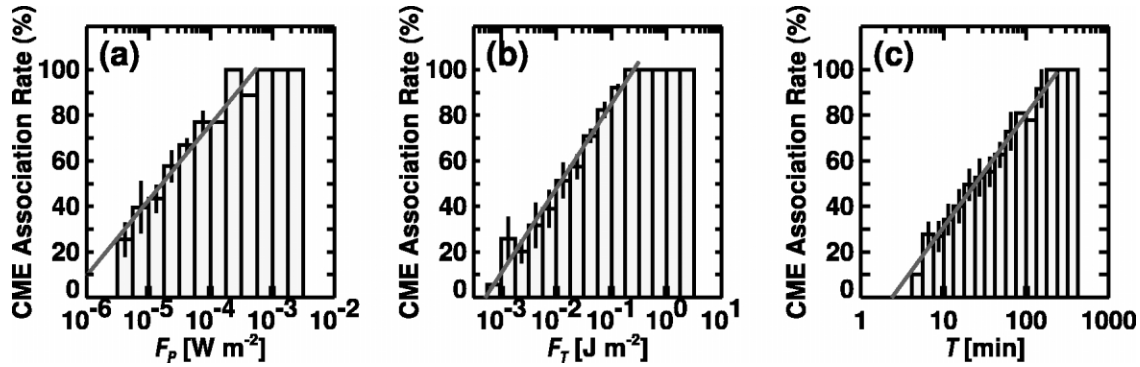[3] Naval Research Laboratory, Washington, DC 20375.

[4] See http://www.sec.noaa.gov/ftpmenu/indices.html.

Fig. 1.—CME association rate as a function of (*a*) X-ray peak flux, (*b*) fluence, and (*c*) duration. The gray straight line is the least-squares fit to the data points.

visible to LASCO. In order to separate the flares with CMEs from those without CMEs as accurately as possible, we eliminated C-class flares with longitudes <60° and M-class flares with longitudes <30°. We also eliminated flares at longitudes >85° because of the possible partial occultation of the X-ray source, resulting in an underestimate of the X-ray flux. Thus, we used the longitude range 0°–85° for X-class flares, 30°–85° for M-class flares, and 60°–85° for C-class flares. There are 5890 flares (above C3.2 level) listed in SGD, but the locations are not listed for ~1800 of them. For the X- and M-class flares, we identified their locations using solar disk images obtained in X-ray, EUV, Hα, and microwave. For C-class flares, we used only those flares with their locations listed in SGD. Applying all the above criteria resulted in 98 X-class, 692 M-class, and 575 C-class flares during the study period.

3. CME ASSOCIATIONS

In order to determine the CME association of flares, we used the *SOHO* LASCO CME Catalog[5] (Yashiro et al. 2004) to find the preliminary CME candidates within a 3 hr time window (90 minutes before and 90 minutes after the onset of X-ray flares). When no candidates were available in the time range, we checked the original LASCO movies to find any unlisted CMEs in the CME catalog. If no CME could be observed due to low-quality LASCO images contaminated by solar energetic particles, we excluded the events from the analysis. The consistency of the association between the flare and CME candidates was examined by viewing both flare and CME movies. Eruptive surface signatures, such as filament eruptions and coronal dimmings, helped ascertain the associations. However, in some cases, we could not determine with confidence whether their association was true or false because some flares had obscure eruptive signatures. In this case, we abandoned the events to give a clear true or false answer of the flare's CME associations and left them as ambiguous associations. This way, we classified all the flares into three categories: flares with definite CME association, flares with uncertain CME association, and flares that definitely lacked CMEs.

Figure 1 shows the CME association rate as a function of X-ray peak flux (Fig. 1*a*), fluence (Fig. 1*b*), and duration (Fig. 1*c*). The CME association rate has an error range obtained from the uncertain flare-CME pairs. Assuming that all of the uncertain events were false, the lower limit of the CME association was determined by dividing the number of definitive events by the total number of flares. Similarly we obtained an upper limit by assuming that all uncertain events were true. We used the middle

of the lower and upper limit as the representative association rate. This is equivalent to assuming that half of the uncertain events had true association.

The CME association rate of X-ray flares clearly increased with their peak flux (Fig. 1*a*). The irregular plot around the X3.0 value ($10^{-3.5}$ W m^{-2}) was due to a small sample size. Only a single flare without CME association reduced the CME association rate from 100% to 89%. The gray line shows the first-order polynomial fit [$R = 33.2(\log F_P + 6.3)$, where R is the CME association rate in percentage and F_P is the peak X-ray flux in units of W m^{-2}]. Note that this equation is invalid for $R \sim 0$. The fit indicates that the CME association rate will be zero below B5 flares, but there are observations that B5 or weaker flares have associated CMEs (N. Gopalswamy & D. Hammer 2006, in preparation).

Figure 1*b* shows a clear increase of CME association rate with the fluence. In our data set, all X-ray flares with fluence ≥0.18 J m^{-2} had associated CMEs. Using the least-squares fitting, we obtained $R = 37.1(\log F_T + 3.3)$, where F_T is the fluence in units of J m^{-2}. Again, this equation is invalid for $R \sim 0$.

Figure 1*c* shows that the CME association rate clearly increased with flare duration. This confirms the well-known fact that long duration (or decay) events are likely to be associated with CMEs (Sheeley et al. 1983; Kay et al. 2003). In our data set, all X-ray flares with duration >180 minutes had associated CMEs. Note that this critical duration (180 minutes) will change if we use different definitions for flare start and end times. We obtain $R = 49.4(\log T - 0.4)$, where T is the duration in minutes. The fit indicates that the CME association rate will be zero at a flare duration of 2.5 minutes. This equation may be unreliable for $R \sim 0$, since the definition of flare start and end may not be good for short-duration flares. It must be noted that the 20,000 X-ray flares recorded in SGD from 1996 to 2005, only 31 (0.15%) flares had their duration <3 minutes.

4. FLARE FREQUENCY DISTRIBUTIONS

There were 5890 X-ray flares (>C3.2 level) from 1996 to 2005, but we could determine the CME associations for selected flares only. Since different selection criteria were applied for C-, M-, and X-class flares (see § 2), we were not able to examine the flare frequency distributions properly from the selected flares. Therefore, we included the deselected flares, assuming that the CME association rates of the deselected flares are the same as those of selected flares. The number of flares with CMEs (N_{WC}) in a bin of Figure 1 was calculated from total flare number (N_{TOT}) in the same bin multiplied by the CME association rate (R): $N_{WC} = N_{TOT}R$.
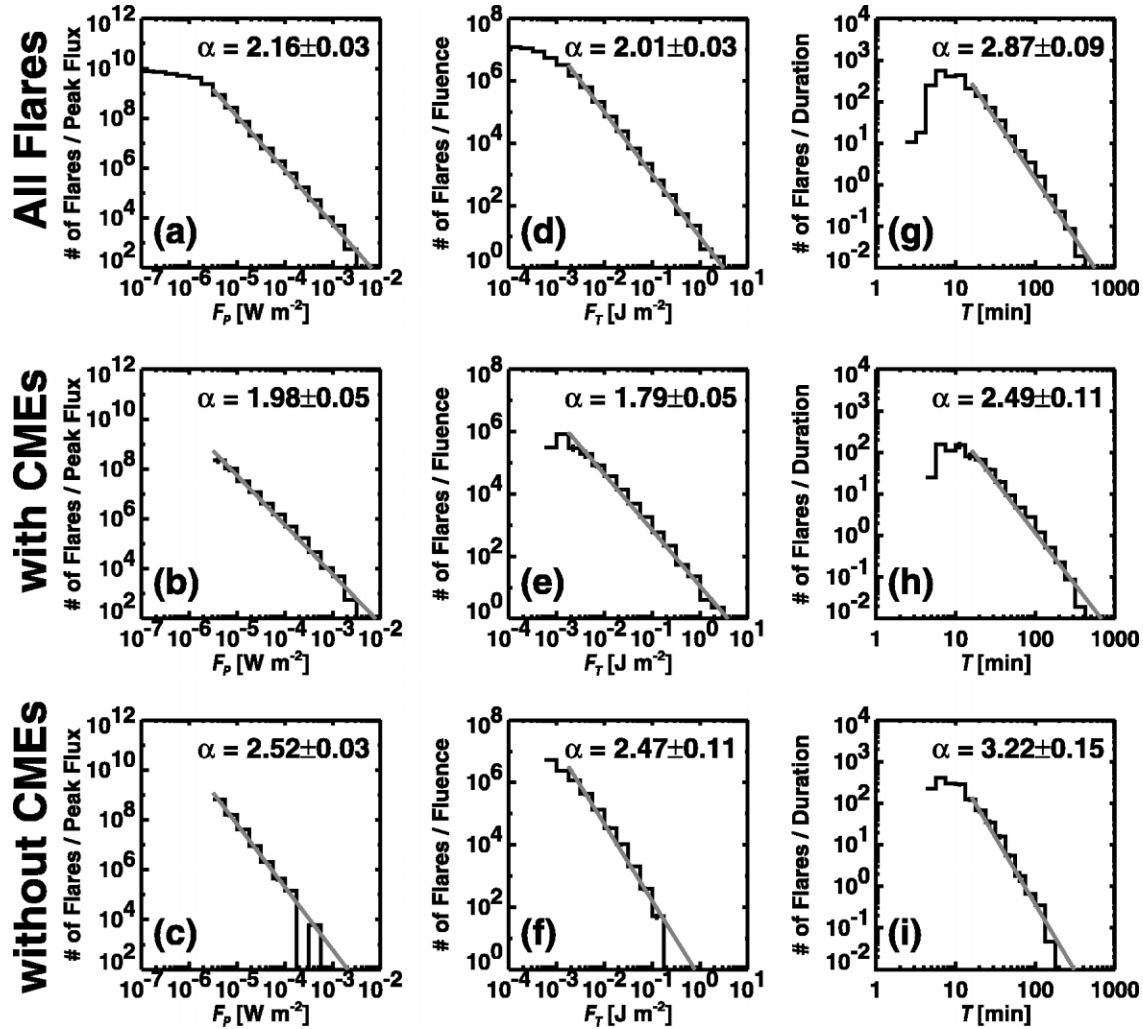
FIG. 2.—Flare frequency distributions as a function of peak flux (*left*), fluence (*center*), and duration (*right*) for all flares (*top*), flares with CMEs (*middle*), and flares without CMEs (*bottom*), respectively. The power-law index α of each distribution is shown in the panel. Flares without CMEs have steeper power-law indices compared to those with CMEs.

For example, there were 743 flares between the values M1.0 and M1.8 ($10^{-5.00}$ W m^{-2} $\leq F_P < 10^{-4.75}$ W m^{-2}), and the CME association rate of this range was 44.1% $\pm$ 6.4%. Then we estimated that the numbers of flares with and without CMEs in this range were 327.7 $\pm$ 47.6 and 415.3 $\pm$ 47.6, respectively. We carried out the same calculation for all the bins in Figure 1 and then obtained the number of flares with and without CMEs.

Veronig et al. (2002) examined almost 50,000 X-ray flares recorded during 1976–2000 and obtained $\alpha = 2.11 \pm 0.13$ for the peak flux, $\alpha = 2.03 \pm 0.09$ for the fluence, and $\alpha = 2.93 \pm 0.12$ for the duration. First we examined frequency distributions for all flares to compare them with the Veronig et al. results. The top panels of Figure 2 are frequency distributions as a function of the peak flux (Fig. 2a), the fluence (Fig. 2d), and the duration (Fig. 2g), showing that all the three distributions are represented by power laws. Using the least-squares method, we obtained a power-law index $\alpha = 2.16 \pm 0.03$ for the peak flux, $\alpha = 2.01 \pm 0.03$ for the fluence, and $\alpha = 2.87 \pm 0.09$ for the duration. The three power-law indices are consistent with the results of Veronig et al. within the error ranges.

The different frequency distributions for flares with and without CMEs are shown in the middle and bottom panels of Figure 2. Note that the error bars are comparable to (or smaller than) the thickness of plotted lines. The left, center, and right panels show the peak flux (Figs. 2b and 2c), the fluence (Figs. 2e and 2f), and the duration (Figs. 2h and 2i), respectively. The distributions are represented by a single power law with the different power-law indices (shown in each panel). For flares with (without) CMEs, we obtained the power-law index $\alpha = 1.98 \pm 0.05$ ($\alpha = 2.52 \pm 0.03$) for the peak flux, $\alpha = 1.79 \pm 0.05$ ($\alpha = 2.47 \pm 0.11$) for the fluence, and $\alpha = 2.49 \pm 0.11$ ($\alpha = 3.22 \pm 0.15$) for the duration. The power-law distributions of all three parameters are steeper for flares without CMEs than those for flares with CMEs.

If flares with and without CMEs have different power-law indices, then combined set of flares should show a double power law. However, we cannot see any indications of a double power law in Figures 2a, 2d, and 2g, because flares with CMEs are predominant in the major ranges. Figure 1a shows that the numbers of flares with and without CMEs are comparable between C5.7 ($10^{-5.25}$ W m^{-2}) and M3.2 ($10^{-4.50}$ W m^{-2}) levels (the CME association rate is from 40% to 60% in this range). Flares without CMEs are predominant below C5.7. However, a significant number of small flares were not detected due to the high X-ray background (during solar maximum, the X-ray background reached M level). Thus, we do not have enough bins to recognize the double power-law distribution.

YASHIRO ET AL.

5. DISCUSSION AND CONCLUSIONS

Since small flares are unlikely to be associated with CMEs, a power-law index obtained from small flares should be similar to that from flares without CMEs. Krucker & Benz (1998) examined the distribution of small flares in the quiet regions observed by the *SOHO* EUV Imaging Telescope and found the power-law index to be 2.3–2.6, which is consistent with our result. However, from X-ray data, Shimizu (1995) found the index to be in the range 1.5–1.6. He examined the distribution of the transient brightenings in active regions observed by the *Yohkoh* soft X−ray telescope. A similar power-law index (1.7–1.8) was found for transient brightenings in the Fe XIX line observed by the *SOHO* Solar Ultraviolet Measurement of Emitted Radiation (Wang et al. 2006). The transient brightenings correspond to the *GOES* B-class flares and below, but the obtained power-law indices were very different from ours. The different temperature response of the three instruments above might have resulted in the different power-law indices. Since the power-law index for the smaller flares is not observationally determined yet, more studies are needed before reaching firm conclusions.

Hudson (1991) showed that smaller flares are able to contribute predominantly to coronal heating when the power-law index α is larger than 2. By separating flares with and without CMEs, we showed that the flare frequency distribution may obey a double power-law distribution. Flares without CMEs predominate at small flare sizes and with $\alpha = 2.47 \pm 0.11$ for fluence, indicating that nanoflares contribute to coronal heating if the frequency distribution keeps the same power-law below the observational limit.

Flares without CMEs are thus a potential source for heating the corona since they do not have energy loss due to CMEs. The CME kinetic energy ranges from 10^{28} to $>10^{32}$ ergs (Gopalswamy 2004), which is generally higher than the flare energy. In flares with CMEs, more than half of the released energy is used by CMEs to escape from the Sun. On the other hand, a lack of CMEs allows the entire released energy to go into flare thermal energy. This is consistent with the observational result that, for a given flare class, flares without CMEs tend to have a higher temperature than those with CMEs (Kay et al. 2003).

CME observations by *SOHO* LASCO over the past 10 years enabled us to perform an extensive statistical analysis of flares with and without CMEs. We examined the CME associations of flares from 1996 to 2005 and found that the CME association rate clearly increases with the flare's peak flux, fluence, and duration. These results have been known from the *Solar Maximum Mission* and Solwind era, but the large sample in our study has shown these relations clearer. The primary result of this Letter is that the power-law index for the distributions of flares without CMEs is much steeper than that for distributions of flares with CMEs. This result supports the possibility that flares without CMEs is a likely source of coronal heating and is consistent with the observation that flares without CMEs have a higher temperature.

REFERENCES

Aschwanden, M. J., Dennis, B. R., & Benz, A. O. 1998, ApJ, 497, 972
Brueckner, G. E., et al. 1995, Sol. Phys., 162, 357
Crosby, N. B., Aschwanden, M. J., & Dennis, B. R. 1993, Sol. Phys., 143, 275
Gopalswamy, N. 2004, in The Sun and the Heliosphere as an Integrated System, ed. G. Poletto & S. Suess (Boston: Kluwer), 201
Gopalswamy, N., Nunes, S., Yashiro, S., & Howard, R. A. 2004, Adv. Space Res., 34, 391
Hudson, H. S. 1991, Sol. Phys., 133, 357
Kahler, S. W. 1992, ARA&A, 30, 113
Kay, H. R. M., Harra, L. K., Matthews, S. A., Culhane, J. L., & Green, L. M. 2003, A&A, 400, 779
Krucker, S., & Benz, A. O. 1998, ApJ, 501, L213
Parker, E. N. 1988, ApJ, 330, 474
Sheeley, N. R., Jr., Howard, R. A., Koomen, M. J., & Michels, D. J. 1983, ApJ, 272, 349

Shimizu, T. 1995, PASJ, 47, 251
St. Cyr, O. C., et al. 2000, J. Geophys. Res., 105, 18169
Veronig, A., Temmer, M., Hanslmeier, A., Otruba, W., & Messerotti, M. 2002, A&A, 382, 1070
Vršnak, B., Maričić, D., Stanger, A. L., & Veronig, A. 2004, Sol. Phys., 225, 355
Wang, T. J., Innes, D. E., & Solanki, S. K. 2006, A&A, 455, 1105
Yashiro, S., Gopalswamy, N., Akiyama, S., Michalek, G., & Howard, R. A. 2005, J. Geophys. Res., 110, A12S05
Yashiro, S., Gopalswamy, N., Michalek, G., St. Cyr, O. C., Plunkett, S. P., Rich, N. B., & Howard, R. A. 2004, J. Geophys. Res., 109, 7105
Zhang, J., Dere, K. P., Howard, R. A., Kundu, M. R., & White, S. M. 2001, ApJ, 559, 452